Environmental Science and Pollution Research (2018) 25:8455–8464
https://doi.org/10.1007/s11356-017-1159-8

RESEARCH ARTICLE

Simultaneous decolorization and desalination of dye wastewater through electrochemical process

Jiaxin Shi[1] · Baogang Zhang[1] · Shuai Liang[1] · Jiaxin Li[1] · Zhijun Wang[1]

Received: 2 October 2017 / Accepted: 26 December 2017 / Published online: 6 January 2018

Abstract

Salt-containing dye wastewater discharged from textile industries causes serious environmental problems. Simultaneous decolorization and desalination of dye wastewater in a laboratory scale electrochemical cell are realized for the first time with boron-doped diamond anode. With initial methyl orange (MO) and NaCl of 50 and 3000 mg L^{-1}, decolorization and desalination efficiencies of 70.2 and 88.7% were achieved after 6-h treatment with applied voltage of 6 V. Increasing applied voltages resulted in the improvements of both color and salt removal, while higher MO concentrations suppressed decolorization and higher NaCl concentration accelerated desalination rate. MO dissociated into anions transferred through the anion exchange membrane into the anode compartment and reacted with the active species as ·OH, H_2O_2, and ClO^- generated in anode compartment, leading to color removal. Component analysis confirmed the destruction of MO, with generation of low molecular weight compounds such as phenol and indole. Ions balance analysis indicated that Cl^- and Na^+ moved to the anode and the cathode compartments respectively through the employed membranes driven by external voltage, realizing salt removal. This study has collectively demonstrated an efficient alternative for satisfactory treatment of salt-containing dye wastewater based on electrochemical technology.

Keywords Decolorization · Desalination · Azo dye · Dye wastewater · Electrochemical process

Introduction

Among various industry types, textile industry is extremely water intensive. Only 85% of coloring matters in textile dyeing process get fixed to cloths, while the remaining 15% of dyes are discarded from dye baths as effluent (Liang et al. 2012; Aravind et al. 2016). This dye wastewater containing synthetic dyes discharged from textile industry exhibits high chrominance and salinity (Zhou et al. 2016; Sun et al. 2009), which would do harm to the growth of aquatic lives and the self-cleaning of waters when releases into water without treatment (Zhang et al. 2016; Bu et al. 2016). Thus, it should be properly treated before discharge, especially for color and salt removal.

A large portion of processes has been devoted to the decolorization of synthetic dyes including physicochemical adsorption (Goel et al. 2011; Mohammadi et al. 2011) and microbiological method (Toro et al. 2013). Adsorption can transfer contaminants from water to another medium which may lead to secondary pollution with difficulties of regenerating used adsorbents (Mrinmoy and Sirshendu 2016), while biological approaches are often limited by the microbial activity and the low biodegradability of dye wastewater (Florêncio et al. 2016; Zhang et al. 2015a, b). Though chemical oxidation processes can realize dye decolorization efficiently (Ma et al. 2014), they are liable to cause secondary pollution or need post-treatment (Alventosa-deLara et al. 2012). Moreover, the generation of carcinogenic compounds and mutagens during chemical oxidation and advanced oxidation processes undoubtedly restricts their application in dye wastewater treatment (Migliorini et al. 2011). In comparison, electrochemical degradation is regarded as a more efficient process to treat dye wastewater with the advantages of simple setup, easy control, ambient operation, and complete degradation (Panizza and

Responsible editor: Bingcai Pan

Electronic supplementary material The online version of this article (https://doi.org/10.1007/s11356-017-1159-8) contains supplementary material, which is available to authorized users.

✉ Baogang Zhang
zbgcugb@gmail.com; baogangzhang@cugb.edu.cn

[1] School of Water Resources and Environment, MOE Key Laboratory of Groundwater Circulation and Environmental Evolution, China University of Geosciences (Beijing), Beijing 100083, People's Republic of China

Oturan 2011; Subba and Venkatarangaiah 2014). For example, MO has been successfully handled in electrochemical system on Pt-Bi/C nanostructured electrode by a square-wave potential method (Li et al. 2013). Electro-Fenton and electrocoagulation have also been utilized to treat dye wastewater (Martínez-Huitle and Brillas 2009), while ion removal is often ignored in decolorization processes.

The profile of the salt concentration in dye wastewater always maintains higher level. The high salinity enhances the mineralization degree of the receiving water and leads to land salinization (Gabelich et al. 2002). Regarding salt removal, reverse osmosis is frequently employed, while membrane fouling has to be faced (Ghanbari et al. 2015). As an emerging technique, capacitive deionization comes in researchers' view, but relatively lower efficiency restricts its practical applications (Porada et al. 2012). Electrodialysis has been proved to be an efficient and versatile method for the applications of drinking water production and wastewater purification because it has many advantages over other methods including strong adaptability, low energy consumption, and easier and low cost of operation and maintenance (Smith 2017). Since NaCl is widely used in the textile industry, electrodialysis has been proved to remove NaCl from textile wastewater efficiently (Chandramowleeswaran and Palanivelu 2006). Azo dyes can also migrate with salt as they can be ionized in electrodialysis systems, and higher applied voltages can result in strong oxidation environment, which facilitate dye decolorization. Thus MO, one of the anionic azo dyes, can also be treated in electrodialysis systems simultaneous with salt removal, exhibiting economic and environmental benefits, while few studies concern roles of oxidizing pollutants accompanied with salt removal in these electrochemical treatments.

In this study, a laboratory scale electrochemical cell in constant-voltage mode with three compartments was constructed and its performance of simultaneous color and salt removal was evaluated. A representative azo dye MO was selected as the target pollutant to simulate salt-containing dye wastewater. Operation factors affecting the performance of above cell were studied. Mechanisms were also investigated, especially for decolorization in aspects of generation and functions of active substances and the degradation products of MO. This study emphasizes the feasibility and effectiveness of electrochemical process to treat dye wastewater for simultaneous color and salt removal satisfactorily.

Experimental section

Materials

A three-compartment laboratory scale electrochemical cell was constructed (Fig. 1), which was divided by a pair of anion and cation exchange membranes (AEM and CEM) purchased from Shanghai Shanghua Water Treatment Materials Co., Ltd., China. Properties of membranes were listed in Table 1, with membrane fluxes of 0.1 mL h^{-1} cm^{-2} MPa^{-1} for both AEM and CEM. They were washed three times with deionized water before use. Anodic and cathodic compartments were in cuboid shape with an effective volume of 288 mL (8 cm × 8 cm × 4.5 cm) and the middle compartment of 96 mL (8 cm × 8 cm × 1.5 cm). The boron-doped diamond (BDD) anode (CONDIAS GmbH, German) with geometric dimension of 2 cm × 2 cm was employed noting its unique advantage in the complete mineralization of organic pollutants (Nava et al. 2014), while cathode was made of carbon plate (Beijing Evergrow Resources Co. Ltd., Beijing, China) with geometric dimension of 4 cm × 4 cm. They were placed tightly to membranes in anodic and cathodic compartments, respectively, with electrode spacing of 2.0 cm and connected by titanium wire with a DC power source during experiment.

Solutions containing 0.01 M Na_2SO_4 was introduced into both anodic and cathodic compartments, while the middle compartment was filled with simulated dye wastewater containing MO ($C_{14}H_{14}N_3O_3SNa$) and salt in the form of NaCl with the settled initial concentration. All chemicals used in this study were analytical grade without further purification.

Experimental procedure

With initial concentrations of MO and NaCl at 50 and 3000 mg L^{-1}, respectively, feasibilities of simultaneous decolorization and desalination of dye wastewater were evaluated in the middle compartment of the electrochemical cell in a 6-h operation cycle with applied voltage of 6 V first. Its behaviors with only MO or NaCl with the same concentration were also evaluated for comparison. Then operation factors affecting performance of the electrochemical cell were studied, including applied voltage (2, 4, 6, and 8 V), initial MO concentration (20, 50, 80, and 100 mg L^{-1}), and initial salt concentration (1000, 3000, and 5000 mg L^{-1}). After that, concentrations of total oxidizing species (TOS) were measured and different scavengers were added respectively to confirm functions of corresponding active species during the MO decolorization process. Isopropanol, 4-hydroxy-2, 2, 6, 6-tetramethylpiperidin 1-oxyl (TEMPOL), and Fe (II)-EDTA were used to remove diffusing ·OH, $\cdot O_2^-$, and H_2O_2, respectively (Guo et al. 2015; Chen et al. 2011). Structural transformation and degradation products of MO were also monitored in the end of typical operation cycle, compared with initial samples. Desalination mechanisms were also investigated by monitoring the distribution and mass balance of Na^+ and Cl^- in different compartments during the operation. The whole experiment was conducted in batch mode at room temperature (22 ± 2 °C). All tests were repeated at least three times at the identical condition and average values were presented.

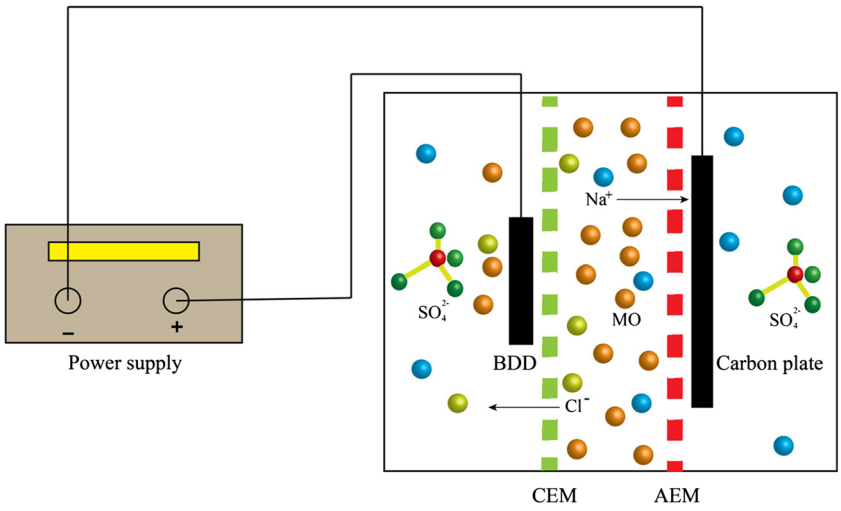

Fig. 1 The laboratory scale electrochemical cell with three compartments employed in present study

Analytical methods

MO concentration was monitored by a UV-vis spectrophotometer (DR 6000, HACH, USA) at 464 nm (Guo et al. 2017). A conductometer (Seven Multi S40, Mettler Toledo, Switzerland) was used to measure the conductivity of simulated dye wastewater to reflect the desalination. The concentrations of Na^+ and Cl^- were determined by Inductively Coupled Plasma Mass Spectrometry (ICP-MS, X Series II, Thermo Fisher Scientific, USA) and ion chromatography (ICS-1100, Thermo Fisher Scientific, USA), respectively. Total organic carbon (TOC) was measured by Multi N/C 3000 TOC analyzer (Analytik Jena AG, Germany) (Zhang et al. 2009). Currents were recorded by a multimeter and energy consumption (EC) was calculated. Current efficiency (CE) was also calculated on the basis of measured TOC (Liang et al. 2017). The concentrations of TOS were determined by N, N-diethyl-p-phenylenediamine (DPD) colorimetric method using a UV-vis spectrophotometer (DR 6000, HACH, USA) (Li et al. 2010), where the added KI was oxidized to I_2 and meantime DPD was oxidized to form a red-violet product by generated I_2 (Reactions (1) and (2)). This measure gave a global concentration of the oxidants, including H_2O_2, O_3, etc.

$$2KI + H_2O_2 \rightarrow I_2 + 2KOH \quad (1)$$

$$I_2 + DPD \rightarrow Red\text{-}violet\ product \quad (2)$$

A wavelength scanning test from 200 to 800 nm was conducted by a UV-visible spectrophotometer (DR 6000, HACH, USA) to reveal the structural transformation of MO during the process. The degradation products were measured by Gas Chromatography-Mass Spectrometric (GC-MS, Trace GC-DSQ, Thermo Fisher, USA) according to (Wang et al. 2015).

Results and discussion

Electrochemical cell performance

With initial concentrations of MO and NaCl at 50 and 3000 mg L^{-1}, respectively, feasibilities of simultaneous decolorization and desalination of dye wastewater were evaluated in the middle compartment of the electrochemical cell in a 6-h

Table 1 Properties of ion exchange membranes used in the present study

Properties	CEM specification	AEM specification
Exchange capacity (mol kg^{-1})	2.0	1.8
Water content (%)	50	40
Resistance of membrane surface (Ω cm^2)	14	18
Thickness (mm)	0.6	0.6
Chemistry stability (pH)	1~13	1~13
Selective penetration (%)	92	94
Permeability of water (mL h^{-1} cm^{-2} MPa^{-1})	0.1	0.1
Coefficient of salt diffusion (mL NaCl cm^{-2} h^{-1})	0.008	0.006

operation cycle with applied voltage of 6 V first, gradual decolorization, and desalination in the middle compartment of the electrochemical cell were simultaneously observed (Fig. 2a). The removal efficiencies of MO reached 70.2% after 6-h treatment, which was comparable to previous study (Alejandra et al. 2017) and showed advantage to foregoing MO degradation studies conducted by anaerobic-aerobic biofilm reactor (Murali et al. 2013). 43.8% of TOC was removed within 6-h operation (Fig. 2b), suggesting partial mineralization of MO took place, which was higher than that realized by peroxymonosulfate-induced reactive oxidants (Lou et al. 2013). Current gradually decreased during the operation (Fig. 2b) and the calculated maximum instantaneous CE and EC were 9.1% and 11.5 kWh m^{-3}, respectively, both of which were comparable with results from undivided electrochemical reactors (Li et al. 2016; Liang et al. 2017). Regarding desalination, satisfactory results were also obtained in our proposed system as the desalination efficiencies reached as high as 88.7% after 6-h operation, also better than previous desalination experiments conducted by electrodialysis (Turek 2003).

The electrochemical system behaviors with only MO or NaCl with the same concentration were also evaluated for comparison to further evaluate its performance. The decolorization efficiencies significantly increased to 95.0% after 6-h treatment when only MO of 50 mg L^{-1} was added into the middle compartment (Fig. 2a). The suppression of decolorization was probably due to the competitive consumption of TOS by Cl^- with MO when MO and NaCl were presented together in simulated dye wastewater (Martinez-Huitle et al. 2016). Furthermore, desalination efficiencies decreased to 66.4% within 6-h operation with sole NaCl in the middle compartment (Fig. 2a), suggesting that the ion migrations were enhanced with the presentation of ionic dye MO due to the improved solution conductivity. Similar phenomenon was also observed that the presence of negatively charged glutamate promoted the migration of Cl^- in the nanofiltration system (Luo and Wan 2006). Therefore, conclusions were drawn that salt-containing dye wastewater could be treated efficiently through this proposed electrochemical process.

Operation factors influences

Effects of applied voltage (2, 4, 6, and 8 V) were studied with initial MO concentration of 50 mg L^{-1} and initial NaCl concentration of 3000 mg L^{-1}, respectively. Both decolorization and desalination efficiencies were improved with applied voltages increasing from 2 to 8 V. Particularly, the decolorization efficiencies increased significantly when applied voltages increased from 4 to 6 V (Fig. 3a). The increased production of TOS under higher applied voltage was responsible for the increase of color removal as previous studies indicated (Ma et al. 2007). More remarkable improvements in aspect of desalination were noted when applied voltage increased from 4 to 6 V (Fig. 3b). The electrical potential is the driving force during ion transport through the membrane and this driving force was strengthened at higher applied voltages as indicated by previous reports (Barakat 2011).

Four gradients of initial MO concentration (20, 50, 80, and 100 mg L^{-1}) were set with initial NaCl concentration of 3000 mg L^{-1} at voltage of 6 V. The decolorization efficiencies decreased gradually during 6-h treatment with the increase of initial MO concentration, from 71.3% with 1.4 mg MO removal at 20 mg L^{-1} to 56.6% with 5.4 mg MO removal at 100 mg L^{-1} (Fig. 3c). The generated intermediate products with MO decomposition could compete with the original dye molecule for the TOS produced by the electrochemical process, thus reducing the decolorization efficiency under higher initial MO concentration (Panizza and Oturan 2011). Desalination efficiencies were slightly affected by variations of initial MO concentration with their values around 88.0% with dialyzed approximate 253.4 mg NaCl in a 6-h operation cycle (Fig. 3d).

Performance of the electrochemical cell was also evaluated under different initial NaCl concentration (1000, 3000, and 5000 mg L^{-1}) with initial MO concentration of 50 mg L^{-1} at applied voltage of 6 V. Similar tendencies of color removal were also observed (Fig. 3e), with around color removal of 70.0% (MO removal of 3.4 mg) under tested conditions in the end of the 6-h operation, indicating that the decolorization was rarely affected by salt profile, similar to the existing report (Buscio et al. 2016). As to salt removal, a significant higher desalination efficiency was exhibited in the first 2 h with the initial NaCl of 5000 mg L^{-1} than that of 1000 and 3000 mg L^{-1} (Fig. 3f). This phenomenon could be attributed to a larger transmembrane concentration gradient that could enhance the transport rate of ions across the membrane (Moya 2017), while their final desalination efficiencies reached similar level of about 88.0% after 6-h treatment, with dialyzed NaCl of 84.8, 253.4, and 422.4 mg, respectively.

Mechanisms investigations

Regarding decolorization in electrochemical systems, indirect electrochemical oxidation induced by the generated active species played important roles (Kariyajjanavar et al. 2011). Levels of TOS concentration in the three compartments of the electrochemical cell without MO addition were monitored. TOS in anode compartment were gradually accumulated as expected, reaching maximum concentration of 28.6 mg L^{-1} at 6 h (Fig. 4), which was measured reflectometrically based on the relationship of absorbance of generated red-violet product through DPD oxidation by active species via I_2/KI mediator. Previous study reported that active species were mainly generated on the anode surface (Li et al. 2010). Nevertheless, TOS in anode

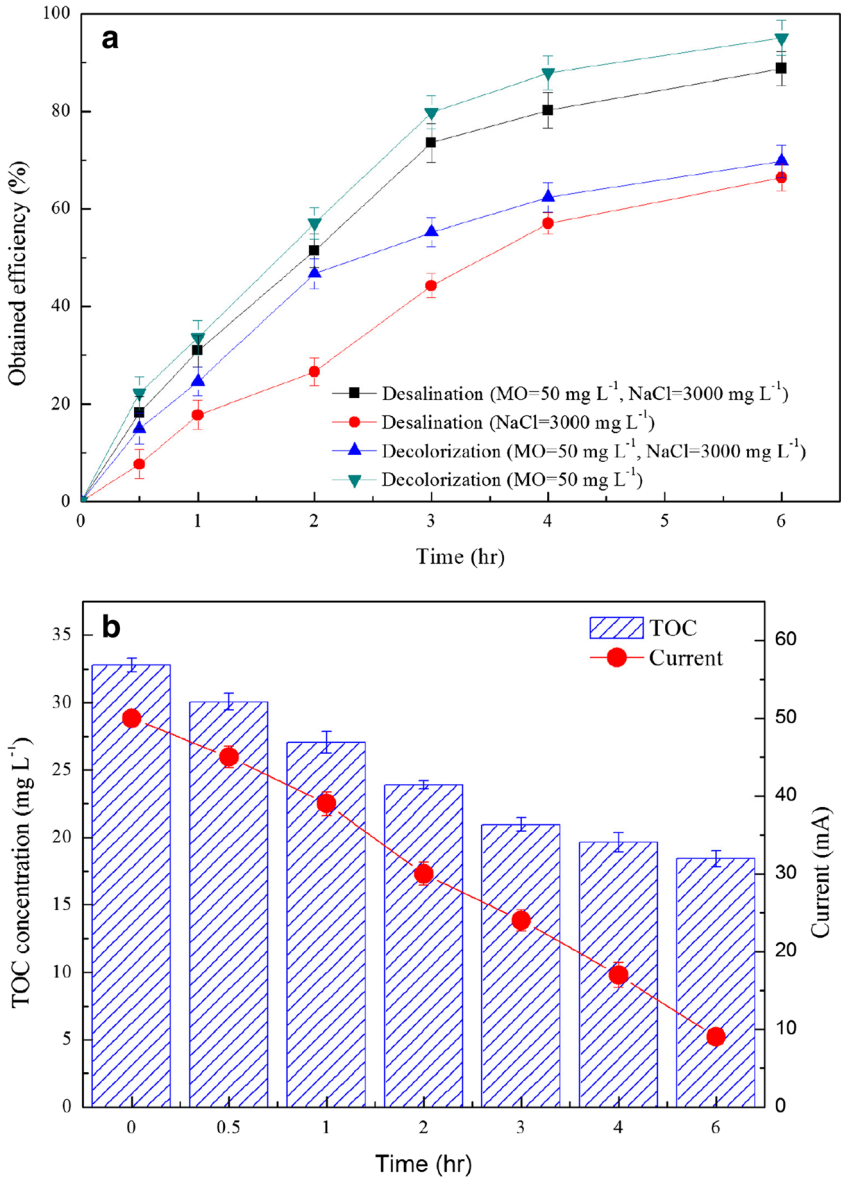

Fig. 2 **a** Decolorization and desalination of dye wastewater in the proposed electrochemical cell and control sets as well as **b** variations of TOC and current in the electrochemical cell during 6-h operation

compartment showed nonlinear growth over time, indicating the concomitant consumption of active species as well as the generation of new ones (Li et al. 2010). Few TOS were detected in the middle compartment and cathode compartment implied that the generated active species on anode surface hardly transferred across membranes used in this study. Therefore, it was elucidated that MO dissociated into anions transferred through the anion exchange membrane into the anode compartment and reacted with the active species generated in anode compartment, leading to color removal. These reactions took place so fast that there were few MO that were accumulated as the anolyte remained transparent during the operation.

Electrochemical processes can generate reactive species such as ·OH, H_2O_2, $\cdot O_2^-$, and so on; the following Reactions (3)–(6) show their formation (Li et al. 2010). Some of them may be responsible for the MO decolorization during the electrochemical process.

$$H_2O \rightarrow \cdot OH + H^+ \quad (3)$$

$$2 \cdot OH \rightarrow H_2O_2 \quad (4)$$

$$OH + H_2O_2 \rightarrow HO_2 \cdot + H_2O \quad (5)$$

$$HO_2 \cdot \rightarrow \cdot O + H^+ \quad (6)$$

To determine the significance of each active specie on the decolorization of MO in the proposed electrochemical cell, different scavengers were added to remove the corresponding active species with initial MO concentration of 50 mg L^{-1} at applied voltage of 6 V. MO decolorization was nearly the same as that without any scavengers when TEMPOL was introduced, indicating that $\cdot O_2^-$ was

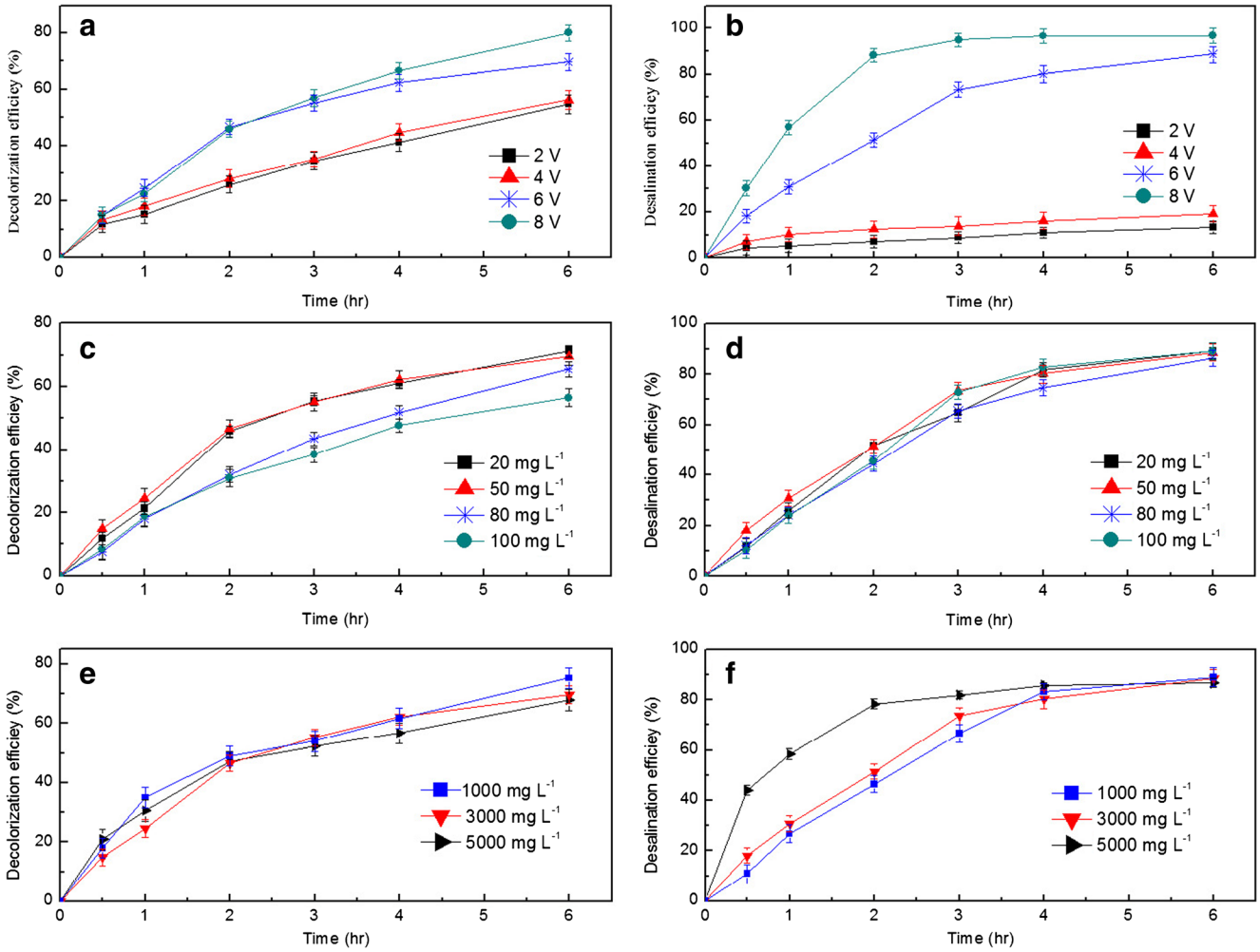

Fig. 3 Effects of different operation factors on decolorization and desalination efficiencies of the electrochemical cell. **a**, **b** applied voltage with initial MO concentration of 50 mg L^{-1} and initial NaCl concentration of 3000 mg L^{-1}; **c**, **d** initial dye concentration with initial NaCl concentration of 3000 mg L^{-1} at voltage of 6 V; **e**, **f** initial salt concentration with initial MO concentration of 50 mg L^{-1} at applied voltage of 6 V

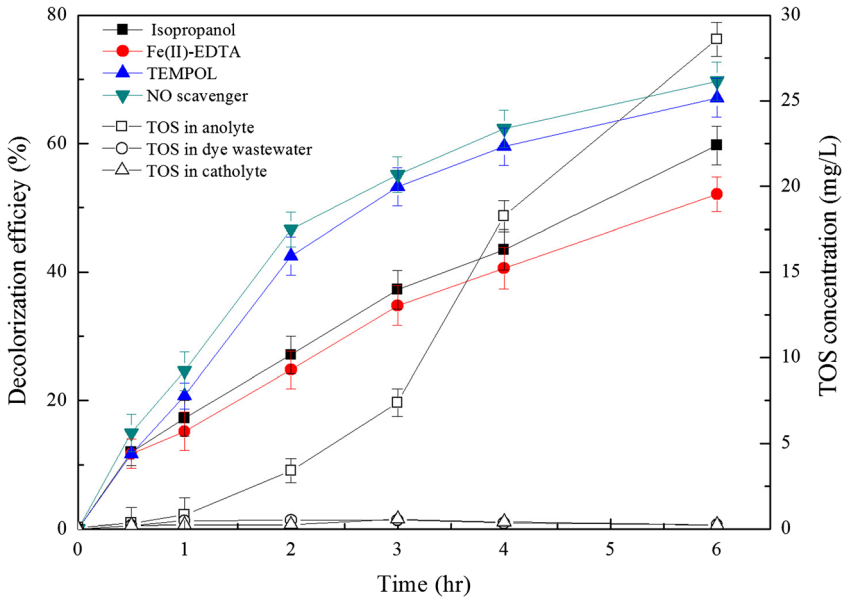

Fig. 4 Decolorization of MO with the presence of different scavengers and accumulations of TOS in three compartments of the electrochemical cell during 6-h operation

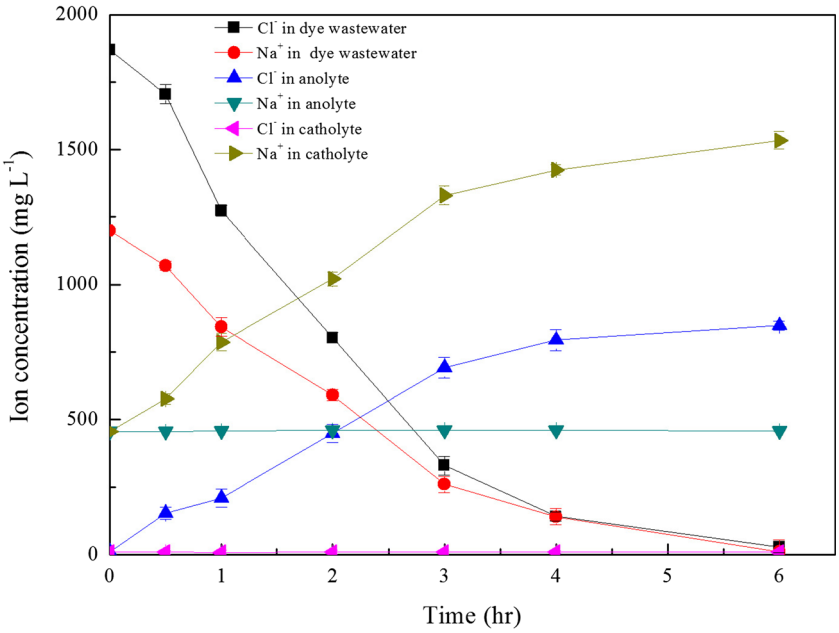

Fig. 5 Concentrations of Na^+ and Cl^- with time in three compartments of the electrochemical cell during 6-h operation

not involved in the decolorization (Fig. 4). Adding isopropanol caused the decrease of decolorization efficiencies of MO to 59.7% in 6 h, which demonstrated that ·OH was definitely involved in this decolorization process. Similar phenomenon was also observed in electrochemical oxidation of Tl(I) with BDD anode (Li et al. 2016). Only 52.1% of MO was decolorized with Fe (II)-EDTA, suggesting that the generated H_2O_2 through Reaction (4) also contributed to MO decolorization. Though H_2O_2 was commonly produced in the cathode of electrochemical systems through oxygen reduction (Zhang et al. 2015a, b), it could also be generated in anode compartments by the dimerization of ·OH and take part in processes for pollutants removal (Yu et al. 2014).

Whereas, simultaneous addition of all scavengers did not completely inhibit the decolorization, which indicated that there were other active substances produced in the anode compartment functioning during decolorization, such as Cl_2 and ClO^- produced from electrochemical oxidation of Cl^- presented in anolyte according to Reactions (7) and (8) (Sala and Gutiérrez-Bouzán 2014). With aids of this active chlorine, MO was further oxidized (Reaction (9)). The positive effect of the generation of active chlorine on the performance of electrochemical oxidation process had been proved (Pereira et al. 2015), especially in the electrochemical decolorization of Acid Red14 (Thiam et al. 2015). Moreover, MO would be intercepted when it went through the anion exchange membrane, causing slight color removal, while the membrane fluxes rarely changed after the whole experiment, further implying that MO decolorization was realized by electrochemical oxidation with the aids of generated active species.

$$2Cl^- \rightarrow Cl_2(aq) + 2e^- \quad (7)$$

$$Cl_2(aq) + H_2O \rightarrow ClO^- + Cl^- + 2H^+ \quad (8)$$

$$MO + ClO^- \rightarrow \textit{Intermediates} \rightarrow CO_2 + Cl^- + H_2O \quad (9)$$

UV-vis spectra scan exhibited the peak at the wavelength of 464 nm decreased continuously with time for the simulated dye wastewater (Fig. S1, Supporting Information), confirming that azo bond was gradually destroyed (Riaz et al. 2014). Meanwhile, the peak at 272 nm corresponding to aromatic ring also declined considerably (Zhang et al. 2006), indicating the simultaneous destructions of the MO molecular structure (Devi et al. 2009). GC/MS was also performed after 6-h operation and more organics with smaller molecule were detected in the exhausted anolyte such as phenol and indole, compared with original simulated dye wastewater (Table S1, Supporting information). Similar intermediate products were also found previously (Li et al. 2013; Cai et al. 2017). Additionally, some organics were also detected in the middle compartment and even in the exhausted catholyte due to their dispersions.

As to desalination, ion balances were monitored. Concentrations of both Cl^- and Na^+ in the middle compartment decreased with time (Fig. 5), thus realizing the satisfactory desalination for the simulated dye wastewater. Driven by external voltage, Cl^- and Na^+ moved to the anode and the cathode compartments through the anion exchange membrane and the cation exchange membrane, respectively, with the observed increase of Cl^- in the anolyte and Na^+ in the

catholyte, respectively (Fig. 5). It was found that migration kinetics of Cl^- and Na^+ followed linear correlation expressed as follows:

$$Cl^- : \ln C_t/C_0 = -0.4696\ t \left(R^2 = 0.9669\right) \quad (10)$$

$$Na^+ : \ln C_t/C_0 = -0.4289\ t \left(R^2 = 0.9708\right) \quad (11)$$

where C_0 and C_t are the initial and remaining concentrations of Na^+ and Cl^-, respectively; k is the removal rate constant.

The desalination rates were undoubtedly reduced due to the gradual decrease of conductivities in the middle compartment (Shabbir et al. 2017). Unlike Na^+, loss of Cl^- was observed (Fig. 5), probably due to the direct electrochemical oxidation of Cl^- on the anode surface (Reaction (7)), which were also reported in the electrophoretic ion exchange desalination system (Shkolnikov et al. 2012). The produced active substances during Cl^- oxidation in this desalination process could be utilized efficiently for MO decolorization, thus achieving the simultaneous decolorization and desalination in one step. Further efforts could be made to combine the proposed electrochemical cell with traditional/emerging techniques, for example, microbial fuel cells as renewable power source and/or for handling dye wastewater simultaneously (Zhang et al. 2009; Guo et al. 2014) to form hybrid systems for practical applications in dye wastewater treatment by further improving the efficiency and reducing the costs.

Conclusions

In this study, we constructed an effective electrochemical cell for simultaneous decolorization and desalination of salt-containing dye wastewater. The decolorization efficiencies of 70.2% and the desalination efficiencies of 88.7% were obtained with applied voltage of 6 V after 6-h electrochemical treatment of solution containing 50 MO and 3000 mg L^{-1} NaCl, respectively. Higher applied voltages improved the performance of both color and salt removal, while higher MO concentrations suppressed decolorization and higher NaCl concentration accelerated desalination rate. MO dissociated into anions transferred into the anode compartment, where the generated active species as ·OH, H_2O_2, and ClO^- contributed to color removal, while salt removal were driven by external voltage based on ions balance analysis. This work further elucidates the possibility for simultaneous decolorization and desalination of salt-containing dye wastewater treatment by electrochemical process.

Funding information This research work was supported by the Fundamental Research Funds for the Central Universities (No. 2652015131).

References

Alejandra CR, Silvia GG, Ricardo S, Juan MPH (2017) Application of electro-Fenton/BDD process for treating tannery wastewaters with industrial dyes. Sep Purif Technol 172:296–302

Alventosa-deLara E, Barredo-Damas S, Alcaina-Miranda MI, Iborra-Clar MI (2012) Ultrafiltration technology with a ceramic membrane for reactive dye removal: optimization of membrane performance. J Hazard Mater 209:492–500

Aravind P, Selvaraj H, Ferro S, Sundaram M (2016) An integrated (electro-and bio-oxidation) approach for remediation of industrial wastewater containing azo-dyes: understanding the degradation mechanism and toxicity assessment. J Hazard Mater 318:203–215. https://doi.org/10.1016/j.jhazmat.2016.07.028

Barakat MA (2011) New trends in removing heavy metals from industrial wastewater. Arab J Chem 4(4):361–377. https://doi.org/10.1016/j.arabjc.2010.07.019

Bu LJ, Shi Z, Zhou SQ (2016) Enhanced degradation of orange g by permanganate with the employment of iron anode. Environ Sci Pollut Res 24:1–7

Buscio V, Maria GJ, Merce V, Victor LG, Marti C, Carmen GB (2016) Reuse of textile dyeing effluents treated with coupled nanofiltration and electrochemical processes. Materials 9(6):490–502. https://doi.org/10.3390/ma9060490

Cai RQ, Zhang BG, Shi JX, Li M, He Z (2017) Rapid photocatalytic decolorization of methyl orange under visible light using VS_4/carbon powder nanocomposites. ACS Sustain Chem Eng 5(9):7690–7699. https://doi.org/10.1021/acssuschemeng.7b01137

Chandramowleeswaran M, Palanivelu K (2006) Treatability studies on textile effluent for total dissolved solids reduction using electrodialysis. Desalination 201(1-3):164–174. https://doi.org/10.1016/j.desal.2005.10.042

Chen YM, AH L, Li Y, Zhang LS, Yip HY, Zhao HJ, An TC, Wong PK (2011) Naturally occurring sphalerite as a novel cost-effective photocatalyst for bacterial disinfection under visible light. Environ Sci Technol 45(13):5689–5695. https://doi.org/10.1021/es200778p

Devi LG, Kumar SG, Reddy KM, Munikrishnappa C (2009) Photo degradation of methyl orange an azo dye by advanced fenton process using zero valent metallic iron: influence of various reaction parameters and its degradation mechanism. J Hazard Mater 164(2-3):459–467. https://doi.org/10.1016/j.jhazmat.2008.08.017

Florêncio T, Araújo KS, Antonelli R, Fornazari AL, Cunha PCR, Bontempo LH, Motheo A, Granato CA, Malpass GRP (2016) Photo-assisted electrochemical degradation of simulated textile effluent coupled with simultaneous chlorine photolysis. Environ Sci Pollut Res 23(19):19292–19301. https://doi.org/10.1007/s11356-016-6912-x

Gabelich CJ, Tran TD, Suffet IH (2002) Electrosorption of inorganic salts from aqueous solution using carbon aerogels. Environ Sci Technol 36(13):3010–3019. https://doi.org/10.1021/es0112745

Ghanbari M, Emadzadeh D, Lau WJ, Matsuura T, Ismail AF (2015) Synthesis and characterization of novel thin film nanocomposite reverse osmosis membranes with improved organic fouling properties for water desalination. RSC Adv 5(27):21268–21276. https://doi.org/10.1039/C4RA16177G

Goel NK, Kumar V, Pahan S, Bhardwaj YK, Sabharwal S (2011) Development of adsorbent from Teflon waste by radiation induced grafting: equilibrium and kinetic adsorption of dyes. J Hazard Mater 193:17–26. https://doi.org/10.1016/j.jhazmat.2011.05.026

Guo W, Feng JL, Song H, Sun JH (2014) Simultaneous bioelectricity generation and decolorization of methyl orange in a two-chambered microbial fuel cell and bacterial diversity. Environ Sci Pollut Res 21(19):11531–11540. https://doi.org/10.1007/s11356-014-3071-9

Guo LQ, Shan C, Liang JL, Ni JR, Tong MP (2015) Bactericidal mechanisms of Au@TNBs under visible light irradiation. Chem Eng J 279:277–285

Guo Y, Wang R, Wang P, Li Y, Wang C (2017) Developing polyetherimide/graphitic carbon nitride floating photocatalyst with good photodegradation performance of methyl orange under light irradiation. Chemosphere 179:84–91. https://doi.org/10.1016/j.chemosphere.2017.03.085

Kariyajjanavar P, Jogttappa N, Nayaka YA (2011) Studies on degradation of reactive textile dyes solution by electrochemical method. J Hazard Mater 190(1-3):952–961. https://doi.org/10.1016/j.jhazmat.2011.04.032

Li HN, Zhu XP, Ni JR (2010) Inactivation of *Escherichia coli* in Na_2SO_4 electrolyte using boron-doped diamond anode. Electrochim Acta 56(1):448–453. https://doi.org/10.1016/j.electacta.2010.08.055

Li SH, Zhao Y, Chu J, Li WW, Yu HQ, Liu G (2013) Electrochemical degradation of methyl orange on Pt-Bi/C nanostructured electrode by a square-wave potential method. Electrochim Acta 92:93–101. https://doi.org/10.1016/j.electacta.2013.01.012

Li YL, Zhang BG, Borthwick AGL, Long YJ (2016) Efficient electrochemical oxidation of thallium (I) in groundwater using boron-doped diamond anode. Electrochim Acta 222:1137–1143. https://doi.org/10.1016/j.electacta.2016.11.085

Liang B, Yao Q, Cheng HY, Cheng SH, Kong FY, Dan C, Guo YQ, Ren NQ, Lee DJ, Wang AJ (2012) Enhanced degradation of azo dye alizarin yellow R in a combined process of iron–carbon microelectrolysis and aerobic bio-contact oxidation. Environ Sci Pollut Res 20:1385–1391

Liang L, Yu FK, An YR, Liu MM, Zhou MH (2017) Preparation of transition metal composite graphite felt cathode for efficient heterogeneous electro-Fenton process. Environ Sci Pollut Res 24(2):1122–1132. https://doi.org/10.1007/s11356-016-7389-3

Lou XY, Guo YG, Xiao DX, Wang ZH, Lu SY, Liu JS (2013) Rapid dye degradation with reactive oxidants generated by; chloride-induced peroxymonosulfate activation. Environ Sci Pollut Res 20(9):6317–6323. https://doi.org/10.1007/s11356-013-1678-x

Luo JQ, Wan YH (2006) Desalination of effluents with highly concentrated salt by nanofiltration: from laboratory to pilot-plant. Desalination 315:91–99

Ma ZH, Wang B, Luo XY (2007) Studies on degradation of methyl orange wastewater by combined electrochemical process. J Hazard Mater 149(2):492–498. https://doi.org/10.1016/j.jhazmat.2007.04.020

Ma SN, Meng JQ, Li JH, Zhang YF, Ni L (2014) Synthesis of catalytic polypropylene membranes enabling visible-light-driven photocatalytic degradation of dyes in water. J Membr Sci 453:221–229. https://doi.org/10.1016/j.memsci.2013.11.021

Martínez-Huitle CA, Brillas E (2009) Decontamination of wastewaters containing synthetic organic dyes by electrochemical methods: a general review. Appl Catal B 87(3-4):105–145. https://doi.org/10.1016/j.apcatb.2008.09.017

Martinez-Huitle CA, Rodrigo MA, Sires I, Scialdone O (2016) Single and coupled electrochemical processes and reactors for the abatement of organic water pollutants: a critical review. Chem Rev 115:13362–13407

Migliorini FL, Braga NA, Alves SA, Lanza MR, Baldan MR, Ferreira NG (2011) Anodic oxidation of wastewater containing the reactive Orange 16 dye using heavily boron-doped diamond electrodes. J Hazard Mater 192(3):1683–1689. https://doi.org/10.1016/j.jhazmat.2011.07.007

Mohammadi N, Khani H, Gupta VK, Amereh E, Agarwal S (2011) Adsorption process of methyl orange dye onto mesoporous carbon material-kinetic and thermodynamic studies. J Colloid Interface Sci 362(2):457–462. https://doi.org/10.1016/j.jcis.2011.06.067

Moya AA (2017) A Nernst-Planck analysis on the contributions of the ionic transport in permeable ion-exchange membranes to the open circuit voltage and the membrane resistance in reverse electrodialysis stacks. Electrochim Acta 238:134–141. https://doi.org/10.1016/j.electacta.2017.04.022

Mrinmoy M, Sirshendu D (2016) Treatment of textile plant effluent by hollow fiber nanofiltration membrane and multi-component steady state modeling. Chem Eng J 285:304–318

Murali V, Ong SA, Ho LN, Wong YS (2013) Evaluation of integrated anaerobic–aerobic biofilm reactor for degradation of azo dye methyl orange. Bioresour Technol 143:104–111. https://doi.org/10.1016/j.biortech.2013.05.122

Nava JL, Sirés I, Brillas E (2014) Electrochemical incineration of indigo. A comparative study between 2d (plate) and 3d (mesh) bdd anodes fitted into a filter-press reactor. Environ Sci Pollut Res 21(14):8485–8492. https://doi.org/10.1007/s11356-014-2781-3

Panizza M, Oturan MA (2011) Degradation of Alizarin Red by electro-Fenton process using a graphite-felt cathode. Electrochim Acta 56(20):7084–7087. https://doi.org/10.1016/j.electacta.2011.05.105

Pereira GF, Rocha-Filho RC, Bocchi N, Biaggio SR (2015) Electrochemical degradation of the herbicide picloram using a filter-press flow reactor with a boron-doped diamond or b-PbO_2 anode. Electrochim Acta 179:588–598. https://doi.org/10.1016/j.electacta.2015.05.134

Porada S, Weinstein L, Dash R, Wal AVD, Bryjak M, Gogosti Y, Biesheuve PM (2012) Water desalination using capacitive deionization with microporous carbon electrodes. ACS Appl Mater Interfaces 4(3):1194–1199. https://doi.org/10.1021/am201683j

Riaz U, Ashraf SM, Aqib M (2014) Microwave-assisted degradation of acid orange using a conjugated polymer, polyaniline, as catalyst. Arab J Chem 7(1):79–86. https://doi.org/10.1016/j.arabjc.2013.07.001

Sala M, Gutiérrez-Bouzán MC (2014) Electrochemical treatment of industrial wastewater and effluent reuse at laboratory and semi-industrial scale. J Clean Prod 65:458–464. https://doi.org/10.1016/j.jclepro.2013.08.006

Shabbir S, Faheem M, Ali N, Kerr PG, Wu YH (2017) Periphyton biofilms: a novel and natural biological system for the effective removal of sulphonated azo dye methyl orange by synergistic mechanism. Chemosphere 167:236–246. https://doi.org/10.1016/j.chemosphere.2016.10.002

Shkolnikov V, Bahga SS, Santiago JG (2012) Desalination and hydrogen, chlorine, and sodium hydroxide production via electrophoretic ion exchange and precipitation. Phys Chem Chem Phys 14(32):11534–11545. https://doi.org/10.1039/c2cp42121f

Smith KC (2017) Theoretical evaluation of electrochemical cell architectures using cation intercalation electrodes for desalination. Electrochim Acta 230:333–341. https://doi.org/10.1016/j.electacta.2017.02.006

Subba RAN, Venkatarangaiah VT (2014) Metal oxide-coated anodes in wastewater treatment. Environ Sci Pollut Res 21(5):3197–3217. https://doi.org/10.1007/s11356-013-2313-6

Sun J, Hu YY, Bi Z, Cao YQ (2009) Simultaneous decolorization of azo dye and bioelectricity generation using a microfiltration membrane air-cathode single-chamber microbial fuel cell. Bioresour Technol 100(13):3185–3192. https://doi.org/10.1016/j.biortech.2009.02.002

Thiam A, Sirés I, Garrido JA, Brillas E (2015) Effect of anions on electrochemical degradation of azo dye Carmoisine (Acid Red 14) using a BDD anode and air-diffusion cathode. Sep Purif Technol 140:43–52. https://doi.org/10.1016/j.seppur.2014.11.012

Toro RD, Celis LB, Cervantes JF, Rangelmendez JR (2013) Enhanced microbial decolorization of methyl red with oxidized carbon fiber as redox mediator. J Hazard Mater 260:967–974. https://doi.org/10.1016/j.jhazmat.2013.06.056

Turek M (2003) Optimization of electrodialytic desalination in diluted solutions. Desalination 153(1-3):383–387. https://doi.org/10.1016/S0011-9164(02)01132-3

Wang ZJ, Zhang BG, Borthwick AGL, Ni JR (2015) Utilization of single-chamber microbial fuel cells as renewable power sources for electrochemical degradation of nitrogen-containing organic compounds. Chem Eng J 280:99–105. https://doi.org/10.1016/j.cej.2015.06.012

Yu XM, Zhou MH, Hu YS, Serrano KG, Yu FK (2014) Recent updates on electrochemical degradation of bio-refractory organic pollutants using BDD anode: a mini review. Environ Sci Pollut Res 21(14): 8417–8431. https://doi.org/10.1007/s11356-014-2820-0

Zhang H, Duan LJ, Zhang DB (2006) Decolorization of methyl orange by ozonation in combination with ultrasonic irradiation. J Hazard Mater 138(1):53–59. https://doi.org/10.1016/j.jhazmat.2006.05.034

Zhang BG, Zhao HZ, Zhou SG, Shi CH, Wang C, Ni JR (2009) A novel UASB-MFC-BAF integrated system for high strength molasses wastewater treatment and bioelectricity generation. Bioresour Technol 100(23):5687–5693. https://doi.org/10.1016/j.biortech.2009.06.045

Zhang JS, Chen SJ, Wang XK (2015a) Sustainable treatment of antibiotic wastewater using combined process of microelectrolysis and struvite crystallization. Water Air Soil Pollut 226(9):315–324. https://doi.org/10.1007/s11270-015-2581-5

Zhang BG, Wang ZJ, Zhou X, Shi CH, Guo HM, Feng CP (2015b) Electrochemical decolorization of methyl orange powered by bio-electricity from single-chamber microbial fuel cells. Bioresour Technol 181:360–362. https://doi.org/10.1016/j.biortech.2015.01.076

Zhang JL, Yu HT, Xie Q, Chen S, Zhang YB (2016) Ceramic membrane separation coupled with catalytic ozonation for tertiary treatment of dyestuff wastewater in a pilot-scale study. Chem Eng J 301:19–26. https://doi.org/10.1016/j.cej.2016.04.148

Zhou KF, Hu XY, Chen BY, Hsueh CC, Zhang Q, Wang JJ, Lin YJ, Chang CT (2016) Synthesized TiO_2/ZSM-5 composites used for the photocatalytic degradation of azo dye: intermediates, reaction pathway, mechanism and bio-toxicity. Appl Surf Sci 383:300–309. https://doi.org/10.1016/j.apsusc.2016.04.155